

Localization in the Quantum Description of the Periodically Perturbed Rotor *)

R. Blümel

Technical University, München, FRG

S. Fishman and M. Griniasti

Dept. of Physics, the Technion, Haifa, Israel

and

U. Smilansky

Dept. of Nuclear Physics, the Weizmann Inst. Rehovot, Israel

Abstract: In this paper we present some recent results concerning localization phenomena in the quantum dynamics of the periodically perturbed rotor. We discuss the response of a planar rotor and of a diatomic molecule to a periodic train of smooth and finite field pulses and show that both cases correspond to an Anderson model on a finite grid. The second topic is the study of the localization properties for the δ -kicked rotor when the kicking strength is large, using the transfer matrix technique.

I. Introduction

In spite of some great progress in our understanding of the quantum dynamics of the kicked rotor,¹⁻¹⁰ the picture we have is still not complete. To set the scene for the ensuing discussion we shall summarize in the following lines some of the established properties of this simple system. The time dependent Hamiltonian is

$$H = \frac{\hbar^2 n^2}{2I} + \hbar k \cos \theta \sum_m \delta(t - mT) \quad (1.1)$$

and the one cycle propagator is

$$U_{nm} = e^{-\frac{1}{2}n^2\tau} (-i)^{n-m} J_{n-m}(k) \quad (1.2)$$

where $\tau = \frac{\hbar T}{I}$ and $k = \hat{k}/\hbar$.

We shall denote by $|\alpha\rangle$ and ω_α the eigenvectors and eigenvalues of the quasi-energy (q.e.) operator G where $U = e^{iG}$. These quasi-energy states have the following properties:

For τ values which are rationally related to 4π the q.e. operator has a regular continuous component in the spectrum with extended eigenstates.⁴⁾ As a consequence, the expectation value of the rotor energy $\frac{\hbar^2 \langle n^2 \rangle}{2I}$ increases quadratically in the number of applied pulses. This is a typical quantum resonance situation.

Recently, it was shown⁵⁾ that there exists a set (of measure zero) of non-resonant τ values for which the q.e. operator has a continuous component, albeit, presumably of a singular continuous nature. The effect of this component on the rotor dynamics is not yet investigated in full.

For generic values of τ , namely excluding these two sets, general analytical results were obtained so far only in the extreme quantum regime $k < \pi$.⁷⁾ By introducing a Hermitian operator W through

$$(1 + iW)(1 - iW)^{-1} = e^{-ik \cos \theta} \quad (1.3)$$

and

$$W = -\tan\left[\frac{1}{2}k \cos \theta\right]$$

The secular equation for the q.e. operator reduces to

$$T_m^{(\alpha)} u_m^{(\alpha)} + \sum_n W_{|m-n|} u_n^{(\alpha)} = 0 \quad (1.4)$$

where

$$\begin{aligned} u_m^{(\alpha)} &= \langle m | (1 - iW)^{-1} | \alpha \rangle \\ T_m^{(\alpha)} &= \tan\left[\frac{1}{2}\left(-\frac{1}{2}m^2\tau + \omega_\alpha\right)\right] \\ W_{|m-n|} &= \langle m | W | n \rangle \end{aligned} \quad (1.5)$$

For $k < \pi$ the matrix elements $W_{|m-n|}$ fall off exponentially in $|m-n|$ since $W(\theta)$ is an analytic function. Therefore, (1.4) is just a tight-binding model in solid state physics, with diagonal elements $T_m^{(\alpha)}$ and hopping matrix elements $W_{|m-n|}$. Its physical properties are similar to those of models where only hopping to nearest neighbors is allowed. If the sequence $T_m^{(\alpha)}$ is random, (1.4) is just the one dimensional Anderson model for localization where all the states are localized. It was argued⁷⁾ that the sequence $T_m^{(\alpha)}$ of (1.5) is effectively random. Consequently, the quasienergy states of (1.1) are exponentially localized in angular momentum space.

*) Lecture Notes in Physics, Vol. 263, T. H. Seligman and H. Nishioka, ed., (Springer 1986).

This explains naturally the bounded and quasi-periodic behaviour of $\langle n^2 \rangle$ in time,^{3,6)} which contrasts with the linear growth expected in the classical theory.

For $k > \pi$ the function $W(\theta)$ is singular and the simple mapping on the Anderson model cannot be used. Numerical calculations¹¹⁾ indicate, however, that the quasienergy states are localized also for $k > \pi$.

In the present paper we would like to extend the above results in two directions. In section II, we shall show that both the resonance and localization phenomena persist even when the δ -kicks are replaced by smooth time dependent pulses, and that one could actually test these effects experimentally by measuring the excitation of rotational bands of diatomic molecules in a microwave field.¹⁰⁾ In section III, we show that the localization mechanism is also effective in the strong interaction domain ($k > \pi$). By using a transfer matrix formulation of the q.e. problem we are able to study the behaviour of the localization length with k .

2. Continuously Driven Rotors - Localization on a Finite Grid.

In this section, we shall deal with two systems which are driven by a train of smooth pulses. The one is the planar rotor, whose discussion will serve to bridge between the schematic δ -kicked planar rotor and the realistic system of a diatomic molecule excited by a microwave field.

The smooth driving pulse can be either chosen as a periodic Gaussian pulse of width σ

$$\Delta^{(\sigma)}(t) = \frac{1}{\sqrt{2\pi\sigma}} \exp\left[-\frac{(t-1/2)^2}{2\sigma^2}\right] \quad 0 \leq t \leq 1 \quad (2.1)$$

or, by truncating the Fourier series for the periodic δ function after N harmonics

$$\Delta^{(N)}(t) = 1 + 2 \sum_{m=1}^N \cos(2m\pi(t-1/2)) \quad (2.2)$$

Both pulse forms are compared in Fig. (1) and the similarity between the functions $\Delta^{(N=7)}$ (t) and $\Delta^{(\sigma=0.03)}$ (t) is apparent. The one cycle propagator is obtained by solving numerically the time dependent Schrödinger equation. The functions $\Delta(t)$ are defined in such a way that we can still use the symbols τ and k to denote the pulse repetition time and its action over a cycle, respectively. Fig. (2) shows the absolute square of the diagonal and first off-diagonal matrix elements of the propagator with $\tau=2$, $k=2$, for the driving pulse $\Delta^{(N=7)}$ (t). The dependence of $|U_{n,n}|^2$ and $|U_{n,n+1}|^2$ on n is characterized by an abrupt change which occurs at $|n| = n_L = 21$ in this case. For $|n| < n_L$, $|U_{n,n}|^2$ and $|U_{n,n+1}|^2$ are almost constant taking the approximate values $|J_0(2)|^2$ and $|J_1(2)|^2$ respectively, which are exactly the matrix elements

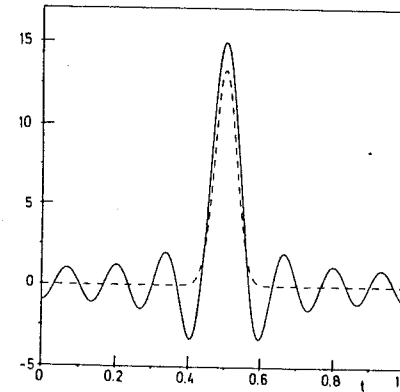


Fig. (1) Possible shapes of a microwave pulse. Broken line: Gaussian form factor $\Delta^{(\sigma=0.03)}(t)$. Full line: Truncated Fourier series for a periodic δ -function $\Delta^{(N=7)}(t)$.

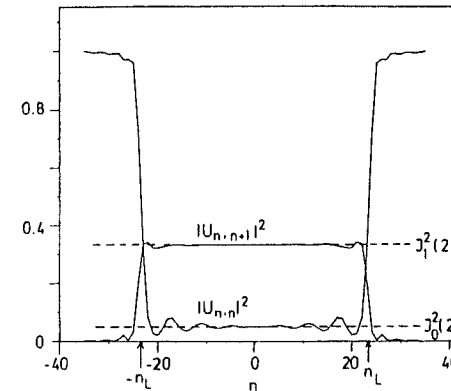


Fig. (2) Absolute squares of diagonal and first off diagonal matrix elements of the one cycle propagator $U(T)$ for $\tau = 2$, $k = 2$ and $\Delta^{(N=7)}(t)$.

of the δ -kicked rotor. For $|n| > n_L$, $|U_{n,n}| \rightarrow 1$ and $|U_{n,n+r}|^2$, $r = 1, 2, \dots$ approach zero, so that the states with $|n| > n_L$ are neither coupled to the states with $|n| < n_L$ nor do they

couple to each other. This phenomenon is due to the fact that the driving field can couple only such states whose transition frequency can be matched by the field frequencies. In our case, the $n \rightarrow n+1$ transition frequency is $n+1/2$ and n_L satisfies

$$n_L + 1/2 = \frac{2\pi}{\tau} N \quad (2.3)$$

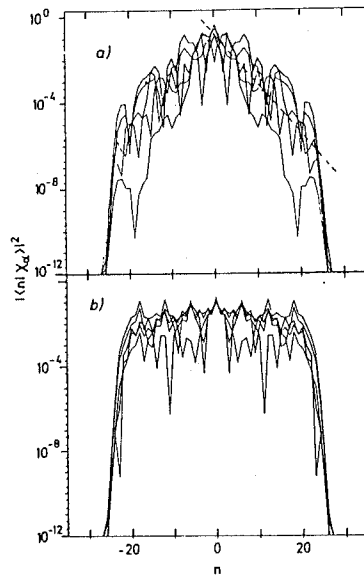


Fig. (3) Some quasi energy states characterized by a large overlap with the rotor ground state $|0\rangle$ for interaction strength $k=2$ and a) $\tau=2$, b) $\tau=\frac{2\pi}{3}$.

The q.e. eigenstates will be correspondingly divided into two categories. The one will contain states which are (trivially) localized on rotor states with $|n| > n_L$, and they will not affect the dynamics as long as the initial state is within the coupled region. The other class will involve the $(2n_L + 1)$ low n states and will couple them strongly as is apparent from the size of $|U_{n,n+1}|^2 \approx 0.33$. Now we may try to see whether there exist extended eigenstates for τ values which are rational multiples of 4π , and if the states become localized for irrational $\tau/4\pi$. Fig. (3) shows the q.e. states which have large overlap with the $n=0$ state for $\tau=2\pi/3$ (resonance)

and $\tau=2$ (off resonance). We observe that the q.e. eigenvectors indeed fall off exponentially and behave as the finite length analogue of the infinite 1-dimensional, Anderson model. The localization length deduced from the mean exponential fall-off (dashed line in Fig. (3a)) is approximately 5 states, while the extended (resonance) states have almost equal probability to be in any state in the $|n| < n_L$ region.

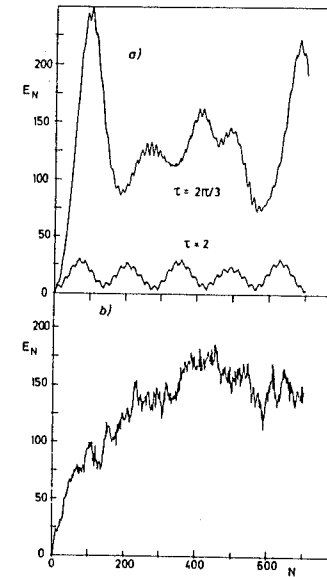


Fig. (4) Average energy of the rotor as a function of time for $k=2$ and $\Delta(t) = \Delta^{(N=\tau)}(t)$. a) Quantum mechanical calculations for the localized ($\tau=2$) and extended ($\tau=\frac{2\pi}{3}$) case. b) Classical calculation ($\tau=2$).

In Fig. (4a), we compare the energy gained by the rotor on and off resonance. The initial quadratic rise in the mean energy on resonance is terminated after some time when all the states in the $|n| < n_L$ region are almost equally populated. The classical result for the energy is shown in Fig. (4b). Here the typical linear increase of the energy with time is terminated after the $|n| \leq n_L$ domain is populated, and there is no further diffusion to $|n| > n_L$ because the classical Chirikov criterion ¹⁾ is only fulfilled for $|n| < n_L$. In the discussion above we have shown that the pictures which characterize the quantum dynamics of the δ -kicked rotor

appear in an analogous fashion in the continuously driven problem. A similar analogy also exists for the classical dynamics, and the similarity persists independently of the detailed shape of the driving pulse. We shall now show that the above considerations can be implemented in an experiment where rotational excitation of diatomic molecules are induced by a train of microwave pulses.

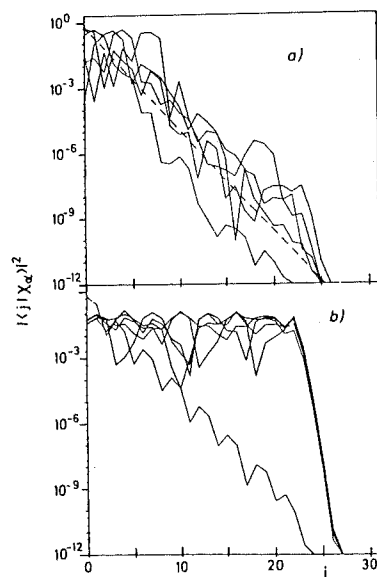


Fig. (5) Some quasi energy states characterized by a large overlap with the molecule ground state $|j=0\rangle$ for interaction strength $k=2$ and a) $\tau=2$, b) $\tau=\frac{2\pi}{3}$.

The Hamiltonian which governs the molecule dynamics is

$$H(t) = \frac{\hbar^2 \vec{J}^2}{2I} + \mu E_0 \cos \theta \Delta(t) \quad (2.4)$$

where \vec{J} is the angular momentum operator in 3 dimensions, I is the moment of inertia of the molecule along an axis perpendicular to the symmetry axis, μ its dipole moment and E_0 is the amplitude of the electric field which is applied in the z direction.

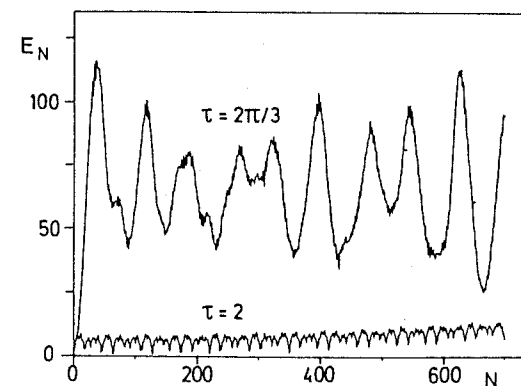


Fig. (6) Average energy of the molecule as a function of time in the localized and extended case.

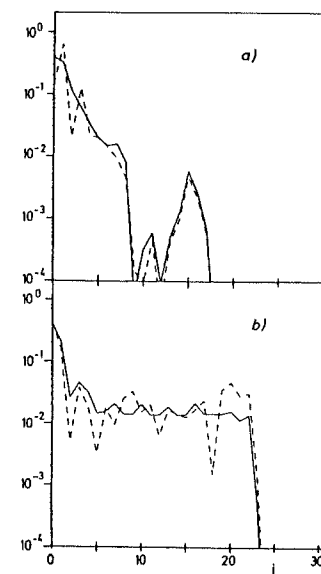


Fig. (7) Occupation probabilities of the angular momentum states of the molecule. Dashed line: "snapshot" after cycle nr. 400. Full line: average of the occupation probabilities from cycle nr. 150 to cycle nr. 200. a) Off resonance. b) On-resonance.

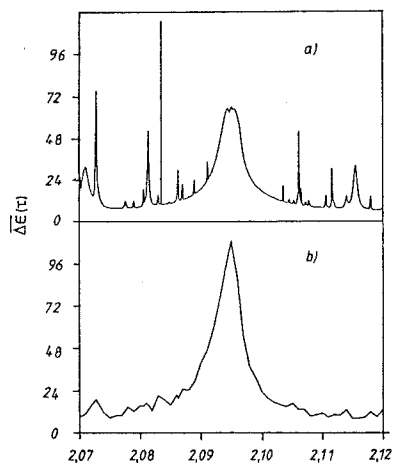


Fig. (8) Average energy gained by the molecule for τ in the vicinity of the resonance at $\tau = \frac{2\pi}{3}$, a) $T_{rot} = 0K$, b) $T_{rot} = 1K$.

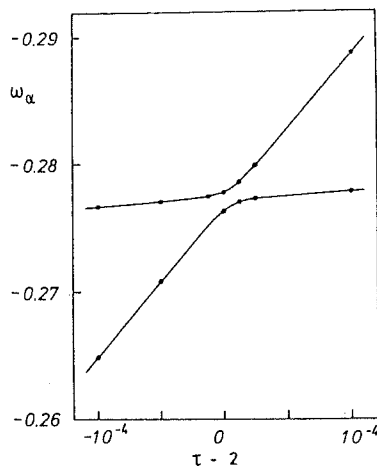


Fig. (9) Avoided crossing of two quasi energies in the vicinity of $\tau = 2$.

The eigenvalues of J^2 are $j(j+1)$, $j=0,1,\dots$ and

$$\langle jm | \cos\theta | j'm' \rangle = \delta_{mm'} (C_j^{(m)} \delta_{j',j-1} + C_{j+1}^{(m)} \delta_{j',j+1})$$

$$C_j^{(m)} = \left[\frac{(j-m)(j+m)}{(2j-1)(2j+1)} \right]^{1/2} \quad (2.5)$$

Thus, the grid of j values is limited to the positive values only, and the rotational energies as well as the dipole matrix elements coincide with the planar rotor values only for large j . Fig. (5) shows the q.e. eigenvectors which have maximal overlap with the ground state for $m=0$ and for off-resonance (a) and resonance (b) conditions. It is apparent that the localization mechanism off resonance is as effective as in the planar case, and the appearance of a single localized state in the resonance case is probably due to an edge effect. The energy absorbed by the molecule is shown in Fig. (6) for the same conditions and the results are very similar to those for the planar rotor. The time averaged probabilities to excite the various j states off and on resonance are shown in Fig. (7) and they exhibit the expected behaviour.

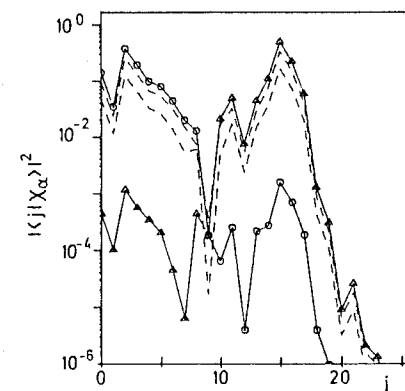


Fig. (10) Nearly degenerate quasi energy states. Full lines: Quasi energy states localized at $|j=2\rangle$ and $|j=15\rangle$ for $\tau = 2 \cdot 10^{-4}$. Dashed lines: The same states for $\tau = 2$.

In order to check in more detail the behaviour of the molecule in the microwave field, we calculated the time-averaged energy transfer as a function of the repetition time τ in the vicinity of the resonance $\tau = \frac{2\pi}{3}$. Fig. (8a) shows the results where the molecule is assumed

to be initially in its ground state. Apart from the resonance structure at $\tau = \frac{2\pi}{3} = 2.094$ we observe several other narrow spikes in the vicinity of the resonance. For τ values ranging from $\tau = 2.07$ to $\tau = 2.12$ none of the spikes occurs on τ values which can be assigned to a value $\frac{2q}{\pi}$ with q smaller than 43. We attribute these structures to the phenomenon of avoided level crossing which is shown in figures (9) and (10). Two q.e. eigenvalues almost cross at $\tau \approx 2$ (see Fig. (9)). The corresponding q.e. eigenstates are shown in Fig. (10) before the crossing occurs (circles and triangles) and at the point of avoided crossing (dashed lines). Before the crossing, the "circle" state is localized around $j=0$ and has a very small overlap with the higher j states. The "triangle" state was localized at $j=15$ having very low overlap with $j=0$. At the crossing point the states must share their structure and indeed the dashed lines show that the rotational states with $j=0$ and $j=15$ have similar overlaps with either q.e. eigenstates, reaching in probability to the 10% level. We thus have a very efficient way to transfer probability between $j=0$ and $j=15$. The region where this mechanism is effective is extremely narrow and hence the small width of the observed spikes. In Fig. (8b), we show the same quantity as in Fig. (8a), but here we assume the molecules to be produced in a beam with rotational temperature of 1K. The absorbed energy should be averaged over the ensemble of different initial j and m values. We see that the proper resonance structure is not affected by this averaging but the avoided crossing effects are smoothed out because of the high sensitivity of the avoided crossing to changes of the matrix elements (due to the presence of molecules with $m \neq 0$) and to the initial j values which involve other q.e. eigenstates. We checked ¹⁰ that molecules like CsI or PbTe possess high dipole moment and are sufficiently heavy, so that an experiment can in principle be conducted with reasonable field strength. We checked the influence of various sources of random noise on the dynamics and found that one could carry out the proposed experiment within present day technology.

3. The Strong Coupling Domain

As was stressed before, the simple method discussed in the previous sections to show the analogy between the q.m. rotor and the Anderson model (see 1.4) is only applicable for $k < \pi$. Here we shall extend the discussion to the domain $k > \pi$ (the strong coupling domain).

The starting point is again the secular equation for the 1 cycle propagator (1.2)

$$\sum_{m=-\infty}^{\infty} J_m(k) a_{n-m}^{(\alpha)} = e^{in^2\tau/2 - iw_\alpha} a_n^{(\alpha)} \quad (3.1)$$

where a phase factor $(+i)^{-m}$ was absorbed into the components $a_m^{(\alpha)}$. The following properties of the Bessel functions will be relevant to the discussion

$$\begin{aligned} a. & \quad \sum_{\nu} J_{\nu}(k) J_{\nu-\nu}(k) = \delta_{\nu 0} \\ b. & \quad J_{\nu}(k) = (-1)^{\nu} J_{-\nu}(k) \\ c. & \quad |J_{\nu}(k)| \sim \begin{cases} (2/\pi k)^{1/2} & |\nu| < k \\ (\frac{1}{2\pi\nu})^{1/2} (ek/2\nu)^{\nu} & |\nu| > k \end{cases} \end{aligned} \quad (3.2)$$

This last property suggests to approximate eq. (3.1) by replacing the infinite sum by a finite sum over the range $|m| \leq b$ where b is an integer larger than k . Consequently the evolution operator (1.2) is a band matrix around the diagonal, with one pseudo random element in each row. Therefore, it has a form similar to the Hamiltonian of the one dimensional Anderson model for localization in a sense similar to the discussion of ref. 7, and localization might be expected to take place in this model as well. In order to establish the localization, the truncated version of eq. (3.1) is posed as a transfer matrix problem in a $2b$ -dimensional vector space.

$$\vec{c}^{(n+1)} = T^{(n)} \vec{c}^{(n)} \quad (3.3)$$

where

$$c_i^{(n)} = a_{n+b-i} \quad i = 1, 2, \dots, 2b$$

and

$$T^{(n)} = \begin{pmatrix} t_1 & \dots & \dots & \dots & t_b & \dots & \dots & \dots & t_{2b} \\ 1 & 0 & \dots & \dots & \dots & \dots & \dots & \dots & 0 \\ 0 & 1 & \dots & \dots & \dots & \dots & \dots & \dots & 0 \\ \vdots & & \ddots & & & & & & \vdots \\ \vdots & & & \ddots & & & & & \vdots \\ 0 & & & & 1 & & & & 0 \\ \vdots & & & & & \ddots & & & \vdots \\ \vdots & & & & & & 1 & & \vdots \\ 0 & \dots & \dots & \dots & 0 & \dots & \dots & 1 & 0 \end{pmatrix} \quad (3.4)$$

with

$$\begin{aligned} t_l^{(n)} &= (-J_{(-b+l)}(k) + \delta_{lb} \exp(in^2\tau/2 - iw_\alpha)) / J_{-l}(k) \quad l = 1, 2, \dots, b \\ t_l^{(n)} &= (-1)^{b-l} t_{2b-l}^{(n)}, \quad 2b > l > b \quad t_{2b}^{(n)} = (-1)^{b+1} \end{aligned} \quad (3.5)$$

The matrices $T^{(n)}$ have the property

$$\Gamma T^{(n)} (-\Gamma^{-1}) = (T^{(n)})^{-1} \quad (3.6)$$

where Γ is the $2b$ dimensional matrix

$$\Gamma = \begin{pmatrix} 0 & \dots & \dots & 0 & 0 & \dots & \dots & 1 \\ \vdots & & & & & & & -1 \\ \vdots & & & & & & & 1 \\ 0 & \dots & \dots & 0 & -1 & 0 & & 0 \\ \vdots & & & & 1 & 0 & & 0 \\ \vdots & & & -1 & & & & \\ \vdots & & & & & & & \\ \vdots & 1 & & & & & & \\ -1 & \dots & \dots & \dots & 0 & & & 0 \end{pmatrix} (-1)^{b+1}$$

from which it follows that:

- (1) $|\det(T^{(n)})| = 1$.
- (2) The eigenvalues of $T^{(n)}$ appear in pairs, if λ is an eigenvalue, there is another eigenvalue λ' such that $|\lambda\lambda'| = 1$.
- (3) The set of matrices having the property (2) is closed under multiplication.

Successive applications of the transfer operation (3.3) expand the volume of ν -dimensional parallelepipeds with $1 \leq \nu \leq b$. The mean expansion rate is the ν -dimensional Lyapunov exponent $\lambda^{(\nu)}$ ¹²⁾

$$\lambda^{(\nu)} = \lim_{N \rightarrow \infty} \frac{1}{N} \ln \frac{\|P^{(N)} \vec{e}_1 \wedge P^{(N)} \vec{e}_2 \wedge \dots \wedge P^{(N)} \vec{e}_\nu\|}{\|\vec{e}_1 \wedge \vec{e}_2 \wedge \dots \wedge \vec{e}_\nu\|} \quad (3.7)$$

where

$$P^{(N)} = \prod_{i=1}^N T^{(i)}$$

and \vec{e}_j are any independent set of ν vectors in $2b$ dimensions. \wedge stands for the exterior product.

If the limit (3.7) exists, we can use the methods of ref. (12) to calculate the $\lambda^{(\nu)}$. The one dimensional Lyapunov exponents may take at most b distinct values which we shall denote by $\{\gamma_i\}$, where $\gamma_1 \geq \gamma_2 \dots \geq \gamma_b \geq 0$;

since

$$\lambda^{(\nu)} = \max_{1 \leq i \leq b} \left\{ \sum_{i=1}^{\nu} \gamma_i \right\} \quad (3.8)$$

we can calculate γ_b once the set of $\lambda^{(\nu)}$ is known for $\nu=1, \dots, b$.

From the properties of the transfer matrix it follows that the one dimensional Lyapunov exponents which govern the contracting subspace are given by $\gamma_i = -\gamma_{2b-i+1}$ $i > b$. The fact that the Lyapunov exponents appear in pairs is due to the symmetry of the problem - the

results should be independent of whether the transfer matrix is applied to the right or to the left.

The minimal positive Lyapunov exponent γ_b determines the localization properties of the q.e. eigenvectors. ¹³⁾ This is just a consequence of the fact that it is associated with the largest length scale in the problem. If it vanishes then there exists an extended eigenvector. Otherwise, the eigenvectors are localized around some value \bar{n} and the localization length $\xi = \gamma_b^{-1}$ determines the mean exponential decay of the amplitudes for n far away from \bar{n} . Before presenting the results, we shall briefly discuss the numerical tests which we performed to convince ourselves of the validity of our approach:

- 1. For any given value of k we calculated the localization length for several values of $b > k$. Convergence, namely, independence of γ_b on b , within a few percent was achieved for $b \geq k+5$, ($k \geq 1$). For such values of b , $|\sum_{|\nu| \leq b} J_\nu^2 - 1| \leq 10^{-3}$.
- 2. Using our numerical procedure to calculate the $2b$ 1-dim. Lyapunov exponents, we verified numerically that the last b exponents are negative, with $\gamma_i = -\gamma_{2b-i+1}$.
- 3. Setting the phase factor in $t_{i=b}^{(n)}$ to 1.0 we obtained for γ_b a very small ($\sim 10^{-6}$) number as expected for the corresponding eigenvector problem.
- 4. We used typically $N \sim 10^4$ iterations in (3.7). We checked ξ after every 10^3 iterations and the values show fluctuations of a few percents about the mean. Based on these observations, we shall quote our results with an uncertainty margin of $\pm 5\%$.
- 5. We calculated the variation of γ_i in the last 10^3 iterations and found it to be of the order of 5% as well.

A key element of the discussion in the preceding chapters was the assumption that the phase factors $e^{im^2\tau/2}$ are sufficiently uncorrelated, to warrant the applicability of the Anderson model to the q.m. rotor. In the same spirit, we shall first display and discuss the localization characteristics for a transfer problem where the phase factors in $t_{i=b}^{(n)}$ are chosen at random, with a uniform distribution on the unit circle. The resulting localization lengths are displayed in Fig. (11) for k values in the range

$1 \leq k \leq 20$. We see that for $k \geq 2$, the data points can be fitted by

$$\xi_R(k) = \xi_0 k^\mu$$

with

$$\begin{aligned} \xi_0 &= 0.517 \pm .014 \\ \mu &= 1.755 \pm .013 \end{aligned} \quad (3.9)$$

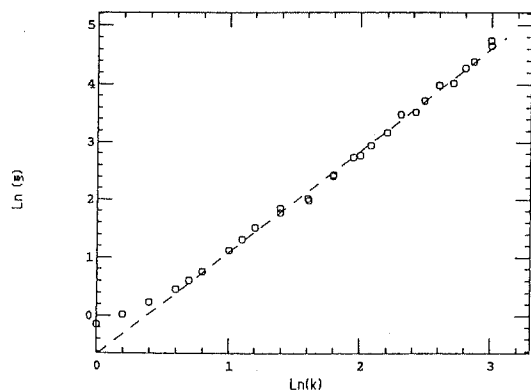


Fig. (11) Calculated $\ln \xi_R(k)$ (dots) vs. $\ln(k)$. The dashed line is the best fit whose parameters are quoted in eq. (3.9).

The parameters and the error bounds were obtained from a χ^2 fit.

In Fig. (12), we show the ratios $\xi(\tau; k)/\xi_R(k)$ for $\tau = 1$ and 2, where $\xi(\tau; k)$ is the localization length calculated with the proper rotor phase. We see that up to a change in the factor ξ_0 , the localization length $\xi(\tau; k)$ seems to oscillate about a mean given by $\xi_R(k)$. The mean of the ratio $\xi(\tau; k)/\xi_R(k)$ is indicated in Fig. (12) by a dashed line. The observed oscillations are rather regular, they are certainly beyond the numerical uncertainty, and at this point we are not able to explain their origin.

We conclude that for the kicked rotor, localization of the quasienergy states persists even in the strong coupling domain. The new feature that this work reveals is that the localization length for the kicked rotor differs from the one calculated on the basis of the assumption that $e^{i\tau n^2/2}$ can be replaced by a random phase¹⁴⁾. However, to a reasonable approximation the random phase calculations reproduce the overall growth of the localization length with k .

Having developed the present tool, the most natural problem to which it should be addressed is the proper semi-classical limit of the rotor, which corresponds to the limit $\tau \rightarrow 0, k \rightarrow \infty$ while $k\tau = K = \text{const}$. Unfortunately, the transfer matrix approach becomes less accurate and more costly in terms of computer resources because (a) with $k \rightarrow \infty$ the dimension of the transfer matrices increase and (b) with $\tau \rightarrow 0$ correlations between the phase factors

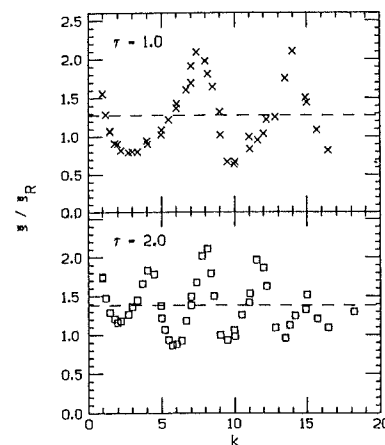


Fig. (12) The ratio $\xi(\tau; k)/\xi_R(k)$ for $\tau = 1$ and 2. The dashed lines give the mean ratio.

survive for $\sim \tau^{-1}$ iterations and therefore the total number of iterations N should be increased proportionally. Thus the approach to the semi-classical limit gets harder since $k\tau^{-1} \sim (1/\hbar)^2$.

After the work was completed, we received a preprint from D.L. Shepelyansky who used a similar method to analyze different aspects of this problem¹⁵⁾.

We would like to thank J. Avron, B. Shapira, R.E. Prange, and D.R. Grempel for useful discussions, and D.L. Shepelyansky for sending us the preprint of his work. The work was supported in part by the U.S.-Israel Binational Science Foundation (BSF).

References:

1. B.V. Chirikov, Phys. Rep. **52**, 263 (1979). B.V. Chirikov, F.M. Izrailev and D.L. Shepelyansky, Sov. Sci. Rev. Sect. **C2**, 209 (1981).
2. G.M. Zaslavsky, Phys. Rep. **80**, 158 (1981).
3. G. Casati, B.V. Chirikov, F.M. Izrailev and J. Ford in: "Stochastic Behaviour in Classical and Hamiltonian Systems", Lecture Notes in Physics, Vol. **93**, p. 334 (Springer

N.Y. (1979)).

4. F.M. Izrailev and D.L. Shepelyansky, *Teor. Mat. Fiz.* 43, 417 (1980), *Theor. Math. Phys.* 43, 553 (80) and *Sov. Phys.-Dokl.* 24, 996 (1979).
5. G. Casati and I. Guarneri, *Commun. Math. Phys.* 95, 121 (1984).
6. T. Hogg and B.A. Huberman, *Phys. Rev. Lett.* 48, 711 (1982) and *Phys. Rev.* A28, 22 (1983).
7. S. Fishman, D.R. Grempel and R.E. Prange, *Phys. Rev. Lett.* 49, 509 (1982), D.R. Grempel, R.E. Prange and S. Fishman, *Phys. Rev.* A29, 1639 (1984).
8. J.D. Hanson, E. Ott, and M. Antonsen, *Phys. Rev.* A29, 819 (1984).
9. S.J. Chang and K.J. Shi *Phys. Rev. Lett.* 55, 269 (1985).
10. R. Blümel, S. Fishman, and U. Smilansky, *J. Chem. Phys.* in Press (1986).
11. M. Feingold, S. Fishman, D.R. Grempel, and R.E. Prange, *Phys. Rev.* B31, 6852 (1985)
12. I. Shimada and T. Nagashima, *Prog. Theor. Phys.* 61, 1605 (1979).
13. This was established rigorously by F. Delyon, Y. Levy, and B. Souillard (to be published) using property (2).
14. This difference was observed in preliminary calculations by M.F. Feingold and S. Fishman, to be published.
15. D.L. Shepelyansky, *Phys. Rev. Lett.* 56, 677 (1986).